recycling

MDPI

Article

Thermal Characterization of Expanded PLA Prototypes Incorporating Grape Stalks and Spruce Bark Residues for Bio-Based Packaging Applications

Niccolò Rimbotti [1,*], Daniele Sarri [1], Jessica Scriva [2], Andrea Pagliai [1], Carolina Perna [1], Federico Rotini [3], Gianluca Bambi [1], Leonardo Conti [1] and Giuseppe Rossi [1]

[1] Department of Agricultural, Alimentary, Environmental and Forestry Sciences, Biosystem Engineering Division-DAGRI, University of Florence, Piazzale delle Cascine 18, 50144 Florence, Italy; daniele.sarri@unifi.it (D.S.); andrea.pagliai@unifi.it (A.P.); carolina.perna@unifi.it (C.P.); gianluca.bambi@unifi.it (G.B.); leonardo.conti@unifi.it (L.C.); giuseppe.rossi@unifi.it (G.R.)
[2] Bluebiloba Startup Innovativa S.r.l., Via C. Salutati 78, 50126 Florence, Italy; jessica.scriva@edu.unifi.it
[3] Department of Industrial Engineering-DIEF, University of Florence, Via di Santa Marta 3, 50139 Florence, Italy; federico.rotini@unifi.it
* Correspondence: niccolo.rimbotti@unifi.it; Tel.: +39-3317845876

Abstract

Bio-based packaging is receiving increasing attention due to the environmental impact of fossil-based plastics. However, its practical implementation requires further evidence on material processing and functional performance. This study evaluated the thermal properties of expanded polylactic acid (E-PLA) prototypes blended with raw, minimally processed agroforestry residues. Specifically, spruce bark and grape stalks were used as waste wood fibers. This study focused primarily on the thermal characterization of the materials by measuring thermal conductivity and resistance. To evaluate the distribution of the two fractions (polymer and fibrous), samples were created with various volumetric ratios between the parts. Simultaneous pressure and microwave heating of the sample were used to stabilize the material. To characterize the raw materials used in this study, bulk density and moisture content were measured. To characterize the mixed materials samples, thermal conductivity and resistance, bulk density, and pressure were measured. To investigate the variables that influence thermal characteristics, statistical analyses such as regression models, ANCOVA, and Spearman correlation were applied. These analyses showed that increasing the biofiber content significantly reduced thermal resistance and increased thermal conductivity. However, negligible effects were observed for the type of fiber used and the duration of the heat treatment. These results describe the thermal properties of blends containing E-PLA and agroforestry residues. The results also show a marked effect of the biofiber content on thermal performance. This study does not provide a comprehensive characterization of the new materials, as it focuses on the prototyping methodology and the laboratory-scale production feasibility of E-PLA/agroforestry-residue prototypes.

Keywords: bio-based; packaging; PLA; agroforestry residues; grape stalks; spruce bark; thermal conductivity; thermal resistance; waste valorization; circular economy

Academic Editor: Mikael Skrifvars

Received: 6 June 2026
Revised: 9 July 2026
Accepted: 13 July 2026
Published: 14 July 2026

1. Introduction

To encourage more efficient and environmentally responsible production systems, scientific research and industry are increasingly re-evaluating the principles of sustainability and environmental protection [1]. The need to mitigate environmental impact stems from

the growing awareness that the intensive use of natural resources and the widespread use of synthetic materials [2] have caused serious global consequences, including impacts on terrestrial ecosystems and broader environmental compartments [3–5]. In response to this emergency, research focuses on developing sustainable alternatives from biodegradable, natural raw materials to reduce waste and revalue end-of-life materials within a circular economy framework [6–8]. In this regard, the packaging sector is one of the most critical sectors, accounting for 40% of global plastic waste, making it the largest plastic production market [9] and a strategic sector for mitigation strategies. According to recent reports, plastic production in 2023 amounted to 413.8 million tons. Of this, 90.4% was fossil-based, 8.7% was mechanically recycled post-consumer plastic, 0.1% was chemically recycled, and 0.7% (3.0 million tons) was bio-based and bio-attributed [10].

Bio-based materials are all those materials obtained, at least in part, from molecules and compounds of biological origin, excluding petroleum or coal derivatives. Consequently, bio-based materials include not only wood fibers, straw, coconut, jute, and cotton, but also polymers composed of or derived from biological products by biomass [11]. Examples of such polymers of biological origin include protein-based films, cellulose and its derivatives, starch-based blends, Polyhydroxyalkanoates (PHA), Polylactic Acid (PLA), and chitosan. These compounds can be used as packaging, coatings, foams, and films, depending on the intended application [12,13]. In packaging applications, bio-based alternatives are receiving increasing attention from the scientific community as an alternative to fossil-based packaging. This focus was particularly on material processing, industrial scalability, sustainability, and end-of-life options [14]. According to the literature, low density, porosity, and thermal resistance are important properties of bio-based insulation materials [15].

Various studies have assessed the viability and quality of different bio-based materials as substitutes for fossil-based ones: The study by Hong et al. demonstrated that a new type of biodegradable foam, composed of 80% corn starch and 20% Polybutylene Adipate Terephthalate (PBAT), reduced thermal conductivity to 0.043 W m^{-1} K^{-1} and improved water resistance and flexibility compared to a foam composed solely of starch [16]. Baniasadi et al., instead, conducted a study on a foam composed of cellulose, pomegranate peel, and Polyethylene Glycol 400 (PEG 400), testing its applicability for cold-chain packaging. The material demonstrated good cohesion without PEG leakage and exhibited a low thermal conductivity of 0.08–0.10 W m^{-1} K^{-1}, a latent heat storage capacity of 65 J g^{-1}, and antibacterial properties [17].

The study by Xie et al. obtained a foam using cellulose obtained from wood pulp. The resulting material achieved a thermal conductivity of 0.0314 W m^{-1} K^{-1}, significantly lower than that of the biofoam reported in the Hong et al. study, demonstrating, in addition to excellent insulating properties, high biodegradability [18]. The study by Kim et al. reports the development of PLA composites strengthened with calcium-crosslinked orange peel biochar, achieving greater combustion resistance, a minimum thermal conductivity of 0.081 W m^{-1} K^{-1}, and good biodegradability [19]. These studies confirm the growing interest in composite materials for packaging and insulation applications, as well as in plant-based foams.

Although biofoam materials can, per se, represent suitable alternatives to conventional plastics, to enhance the properties and the performance of the materials, biofoams can be combined with other organic components. In particular, from a circular economy perspective, it was appropriate to consider elements that are usually considered waste. A recent study by Blasi et al. in 2023 highlighted the potential of lignocellulosic agricultural residues for producing bioplastics, bio-based composites, and other high-value products [20]. Taking these elements into account, fibers such as spruce bark and grape stalks can be considered viable alternatives.

According to San Martín et al., most grape stalks from winemaking are not valorized, are destined for composting, or are discarded in open vineyard areas [21]. Previous studies have explored the use of viticulture byproducts in the construction industry. In particular, grape stalks and crushed grape stalks have been used as components for insulation panels. In the study by Badouard et al., grape stalks were used along with 20% potato starch as a binder. Although this study addresses a different topic than the one examined here, it demonstrates the potential of grape stalks as components of a stable, bio-based aggregate [22].

Within the spruce wood processing industry, the bark was primarily used as a low-value energy source. A secondary, but equally common, use of spruce bark was in horticulture as a component of growing media, as a mulch, or for composting [23]. Previous studies have investigated spruce bark as a raw material for thermal insulation panels, but unlike the previous study on grape stalks, it was used without a binder. Although this research addresses a different topic, it demonstrates the potential thermal properties of spruce bark, supporting its use as a technical reference for the present feasibility study [24].

On this basis, the present study had the following objectives:

1. To use plant fibers (spruce bark and grape stalks), in their raw, macroscopic state to explore the potential of minimally altered fibers for producing a new type of biopackaging.
2. To evaluate the thermal response of the mixes between the fibers and assess their preliminary suitability for agri-food packaging applications through comparison with the most commercially used plastic alternative.
3. To define the ideal ratios for a combination of bio-based polymers and agroforestry residues as lignocellulosic fibers from a thermal point of view.

2. Materials and Methods

For the experiments conducted in this study, a Radwag WPS 50 SX/1 thermobalance produced by Radwag Balances and Scales (Radwag Balances and Scales, Radom, Poland) was used to quantify the moisture content of biomass. A metal cylinder and a Kern Pres 4200-2M analytical balance (Kern & Sohn, Balingen, Germany) with a resolution of 0.01 g were used to determine the bulk density of the raw materials.

Packaging samples were prepared using a parallelepiped wooden mold and compacted with an OMCN 154 hydraulic press (OMCN S.p.A., Bergamo, Italy) samples, and a WIKA digital pressure gauge CPG500 (WIKA, Klingenberg am Main, Germany) to detect the pressure of hydraulic oil. Finally, a NE-1853 heavy-duty microwave heating unit (Panasonic, Kadoma, Japan) was used to thermally treat the specimens, and a Thermtest HFM-100 heat flow meter (Thermtest, Hanwell, NB, Canada) was used to measure thermal conductivity. The Kern Pres analytical balance was used to analyze the weight of the polymeric and fiber parts of the samples. The analysis process described in this section is schematized in the workflow shown in Figure 1.

2.1. Materials Analysis

The raw materials used in this study include agricultural and forestry biomass waste. In particular, the agricultural materials were grape stalks from *Vitis vinifera* (L., 1753), cultivar Sangiovese, and spruce bark from *Picea abies* (H. Karst., 1881). These lignocellulosic components were incorporated into an expanded biopolymer matrix as particulates.

Each material was subsequently analyzed for moisture content and bulk density. The moisture content (MC) of the sample was expressed in the following Formula (1). In this

equation the initial mass of the sample before drying, measured in grams, is denoted by m(t), while ms is the dry mass after drying [25]:

$$MC = \frac{\mathrm{m(t)} - ms}{\mathrm{ms}} * 100 \quad (1)$$

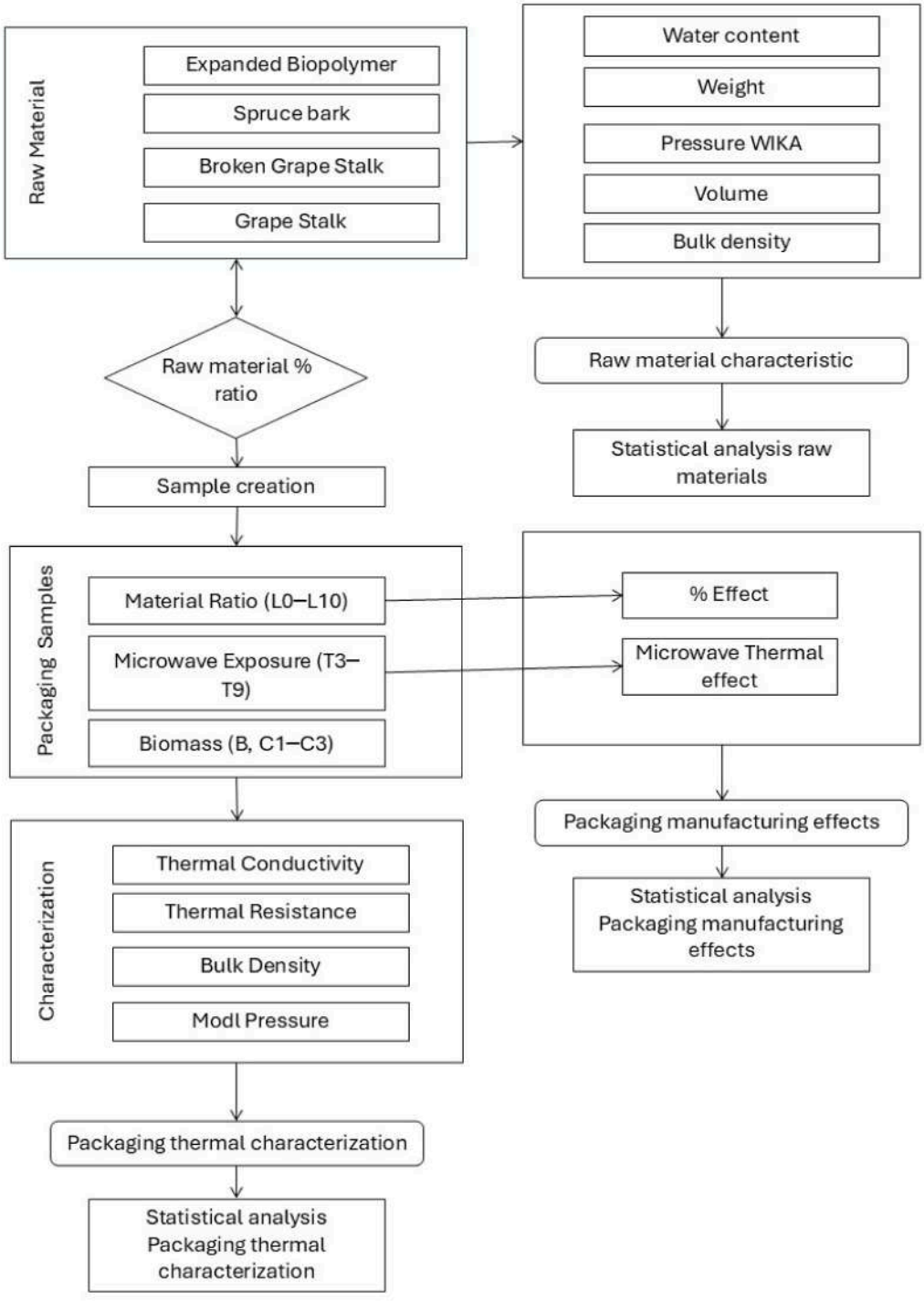

Figure 1. A representative flowchart of the workflow for raw material characterization, prototyping, and thermal characterization. The testing procedures are outlined for each of the three macro-sections.

The moisture content of the raw materials was measured using a Radwag WPS 50 SX/1 thermobalance. The sample was placed in the thermobalance at room temperature and heated to 120 °C to achieve complete drying. Complete drying was assessed by monitoring

the sample weight. Once a constant weight was reached, the instrument produced an acoustic signal to warn the operator that the measurement was complete. Moisture was calculated using a thermobalance as the difference between the initial and final weights.

To measure the bulk density of the raw materials, a methodology adapted from Chevanan et al.'s study was used. The compaction behavior and apparent mass of biomass were evaluated using cylindrical metal containers and a Universal Testing Machine (UTM). In the present study, a similar method was used, using a metal cylinder with an internal diameter of 127.1 mm, a height of 150 mm, and a wall thickness of 6.3 mm [26]. In this analysis, to evaluate the sample volume, a caliper was used to measure the height of the specimen by calculating the difference between the total height of the cylinder and the distance of the cap from the top of the cylinder itself. This difference was then multiplied by the base area to obtain the volume of the samples under pressure.

The experiment was carried out by inserting a known weight of each material and applying pressure, with the readings recorded by Kern Pres analytical balance and WIKA digital pressure gauge. The mass and pressure values applied are reported in the following sections. The bulk density was derived from the mass-to-volume ratio, calculated by determining the volume occupied by the compressed mass. Bulk density (ρb) according to Chevanan et al. study, was obtained from the ratio between the mass (m) and the volume (V) through the following Equation (2) [26]:

$$\rho b = \frac{m}{V} \tag{2}$$

To limit variability across the tests performed in this study, the iron cylinder and the parallelepiped wooden molds had similar base areas: 12,686 mm^2 for the cylindrical mold used for the raw materials and 12,705 mm^2 for the parallelepiped mold used for the E-PLA blends. The parallelepiped wooden mold, introduced at the beginning of this section, is discussed in the manufacturing section below. For the same reason, similar compressed sample thicknesses were selected for the raw materials and biopackaging experiment samples. Pressure inside the cylinder was gradually increased by manually pumping oil to achieve the desired sample density.

These values recorded by the digital pressure gauge (P1) were then converted to obtain the pressure exerted by the cylinder cap on the material inside it (P2). This estimate was performed from the ratio between the piston striking area (A1) and the area of the metal cylinder cap (A2) using the following Equation (3):

$$P2 = P1 * \frac{\mathrm{A1}}{\mathrm{A2}} \tag{3}$$

2.1.1. Material: Expanded Biopolymer

An example of a bioplastic was polylactic acid (PLA), a synthetic polymer of biological origin obtained from starch and sugars extracted from corn, wheat, or potatoes. PLA was widely applied and studied for packaging, thanks to its mechanical properties, which can be competitive with those of conventional polymers, its biological origin, its biodegradability under appropriate conditions and its processability [27]. PLA was currently used in various industries, including food packaging, the production of granular expanded biopolymers, and the production of biodegradable films. The literature includes studies on the use of PLA blended with waste plant fibers. According to a study by Saccani A. et al., post-industrial PLA, derived from film production, can be mixed with coffee silver skins from a blend of Arabica and Robusta varieties to obtain a sustainable composite material [28].

The study addresses the development of a protocol for producing bio-based packaging prototypes from plant biomass waste and PLA, on their thermal performance. Thermal

conductivity and resistance were used as the primary indicators of the samples' suitability for protective packaging.

For this study, we used a particulate foam made of expanded polylactic acid (Bio-Foam™), produced by Bewi (Bewi srl, Bornem, Belgium), as the polymer matrix. The material consists of expanded PLA (E-PLA) beads with a diameter of 3 mm, suitable for thermal bonding [29]. The bulk density characterization was carried out by inserting a precise amount of material, specifically 30 g of E-PLA, inside the metal cylinder mold. To obtain a density inside the manufacturer's specified density range of 25 kg/m^3 to 60 kg/m^3 [29], a pressure of 450 $\pm$ 10 kPa was applied following a preliminary test. The test consisted of creating samples at different pressures, ranging from 1000 to 300 kPa. At each 100 kPa interval, a new sample consisting of three replicas was created. For each replica created with specific pressure, the material configuration and aggregation were visually assessed. The correct aggregation was considered the one that allowed the samples to retain their shape during handling without compromising the structural integrity of the base materials. The pressures that yielded the best results were 500 kPa and 400 kPa; consequently, the pressure was set to 450 $\pm$ 10 kPa. In order to obtain the pressure of the E-PLA sample inside the mold we applied the equation previously introduced (3), obtaining a result of 44.6 $\pm$ 1 kPa.

2.1.2. Material: Spruce Bark

The material was collected in the Val di Fiemme, Trentino-Alto Adige region, Italy [46.2874343° N, 11.4666459° E], following a forestry operation and subsequently processed in a sawmill. The bark has not been classified by size due to its high degree of morphological heterogeneity. This characteristic may influence its behavior regarding vapor absorption and water storage [30]. The only alteration made to the raw material, required exclusively for use in the present study, consisted of the reduction in the components to a length less than 20 mm. In this case, 279 g of material was used to determine the bulk density. For spruce bark, the digital pressure gauge reading was set to 760 $\pm$ 10 kPa, corresponding to a pressure exerted by the cylinder cap on the samples of 75.3 $\pm$ 1 kPa. In this test, a different pressure was applied because it was observed that woody biomass required a higher applied pressure to obtain cohesive specimens, consistently with previous evidence that biomass materials can show different compaction and elastic responses under load [31].

2.1.3. Material: Grape Stalks

The grape stalks were sourced from winemaking cooperatives in Tuscany, Italy [43.5180936° N, 11.2939093° E]. To evaluate the influence of shoot morphology on the apparent cohesion and structure of the samples, both manually broken and whole stalks were used. Each type was assigned a distinct identification code.

The bulk density of the stalks under load was determined using the same methodology described at the beginning of this section. In this case, 233 g of material was used to determine the bulk density of both whole and broken stalks. For both grape stalks, the digital pressure gauge reading was set to 760 $\pm$ 10 kPa, following the same pressure-selection procedure used for E-PLA. This value corresponds to a pressure exerted by the cylinder cap on the samples of 75.3 $\pm$ 1 kPa.

2.2. Experimental Design and Specimen Preparation

The packaging solutions examined in this paper consisted of a mixture of E-PLA and agricultural and forestry biomass waste, namely grape stalks and wood barks. The sample creation process followed the workflow shown in Figure 2.

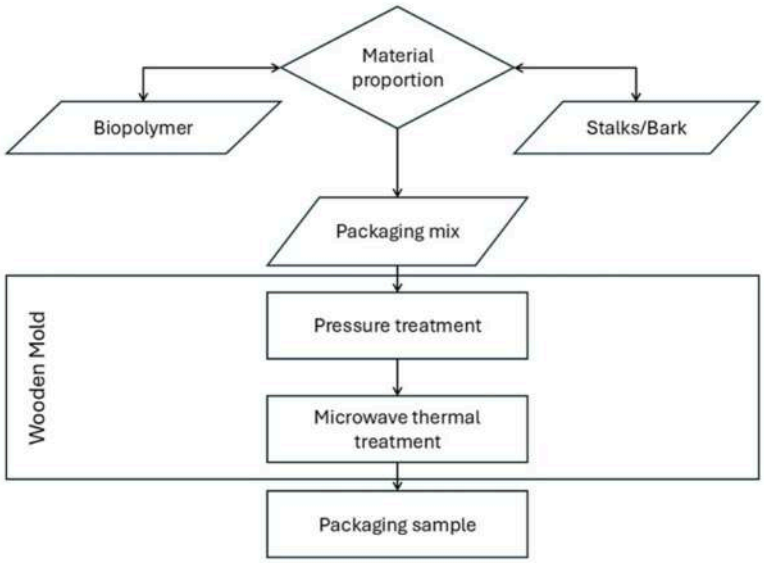

Figure 2. Flowchart of the process for preparing blend samples containing E-PLA and waste fibers. In the first phase, the polymer-fiber blend is created and inserted into the mold. This is followed by the compression and heat treatment phases of the material to obtain the packaging sample.

2.2.1. Material Ratios and Microwave Exposure Duration

Such pressure reduces macropores and ensures proper compression of the bioplastic when mixed with the biofiber. The formulation of the samples was defined by progressively varying the plant fiber-to-biopolymer ratio, as reported in Table 1. In particular, eight samples identified by the codes L0 to L10 were prepared and characterized by different volumetric percentages of the two components. Sample L0 consists exclusively of biopolymer (100%) without the addition of plant fiber (Figure 3), while sample L10 contains only plant fiber (100%) without a polymer matrix. The intermediate samples exhibit a gradual composition shift, with the plant fiber fraction increasing from 10% to 70% and the biopolymer fraction decreasing from 90% to 30%. This experimental design allowed to evaluate the influence of the plant fiber content on the properties of the composite material.

Table 1. The volumetric ratios between waste plant fiber and expanded biopolymer in the specimens are indicated with identification codes.

Code	Plant Fiber (%)	Biopolymer (%)
L0	0	100
L1	10	90
L2	20	80
L3	30	70
L4	40	60
L6	60	40
L7	70	30
L10	100	0

The unique code Lx was used to indicate the volumetric percentage ratios between expanded biopolymer (B) and plant fibers (C), where "x" indicates the percentage of biomass waste present (Table 1).

The standard microwave exposure duration for all samples was set to 6 min because the expanded biopolymer sample showed neither melted portions from excessive heating nor loosened portions from insufficient exposure. Additionally, the trials examined other exposure times in order to evaluate the distinct properties of biofibers. The unique Tx code

identifies the thermal treatment level for the specimens, while the corresponding exposure times are reported in Table 2. The heat treatment was performed by subjecting the material to microwave radiation at 2.45 GHz and a nominal power of 720 W.

Figure 3. Image of the sample made entirely of expanded PLA (E-PLA). It was produced at a WIKA pressure gauge reading of 450 ± 10 kPa and subjected to a 6 min microwave heat treatment.

Table 2. Codes related to the different microwave heat treatment times used in this study.

Code	Microwave Exposure (min)
T3	6
T5	8
T7	10
T9	12

To ensure easy identification of the experimental variables, the specimens produced were named according to a specific convention. Each name was composed of a sequence of letters and numbers in the format Tx_Cx_Lx. In this format, T denotes the thermal treatment time, C the biomass waste sample used and L the level of the volumetric ratio considered. For the reference, set internally by E-PLA, the letter C was replaced by the letter B. The experimental conditions for each test piece can be accurately traced using this naming system.

2.2.2. Manufacturing of the Parallelepiped Mold for Packaging

Wooden molds were created to make specimens measuring 121 mm in width, 105 mm in length, and 55 mm in height. The choice of mold material was based on the need for microwave resistance. The choice of dimensions, however, was related to the methodology used to estimate the bulk density. The base of the metal cylinder and the wooden mold are almost identical. The mold dimensions were 138 mm high, 173 mm wide, and 157 mm long, with a wall thickness of 26 mm. The mold was closed by a base and a cap, both with the same wall thickness, measuring 121 mm wide and 105 mm long (Figure 4).

To ensure accurate adherence to the proportions established for each mixture, the materials were weighed using a Kern Pres 4200-2M laboratory analytical balance. Manual mixing was used because the polymer component has a significantly lower density than the biofiber. Manual mixing, in fact, allows for greater control over the layering and distribution of the material. To verify this mixing, the samples were sectioned. The mixture was placed inside the wooden mold and then closed with the appropriate lid. The test was subsequently compressed using an OMCN 154 hydraulic press until the expected volume of 0.698 L was reached, and the lid was locked in its final position with pins. Finally, the test piece was subjected to a thermal cycle in a 720 W microwave heating unit.

Figure 4. Image showing the parallelepiped wooden mold used during the experiments. The mold dimensions were 138 mm high, 173 mm wide, and 157 mm long, with a wall thickness of 26 mm. The mold was closed by a base and a cap, both with the same wall thickness, measuring 121 mm wide and 105 mm long.

2.3. Methodology of Thermal Characterization

The thermal properties of the samples were evaluated using an HFM-100 Thermtest heat flow meter. The instrument operated on the principle of thermal flow measurement described in ASTM C518 and ISO 8301 [32,33]. These standards provide a standardized reference for the steady-state measurement of heat transfer properties in insulating materials. The sample was placed between two plates, one for cooling to 10 °C and the other for heating to 30 °C, during the measurement process. The bottom (cooling) plate was fixed, while the top (heating) plate was movable with sensors that lowered it until it contacted the top of the sample. Once the sample was locked, the measurement phase began. Both plates were equipped with sensors that monitor heat flux generated by temperature differences. The measurement continued until a steady-state heat flux was reached, allowing the thermal conductivity (K) and thermal resistance (R) of the sample to be calculated, expressed in W m^{-1} K^{-1} and m^2 K W^{-1}, respectively. Thermal conductivity (k), according to the study conducted by Baniasadi et al., was obtained through the following Equation (4) [15]:

$$k = \frac{Q * L}{A * \Delta T} \tag{4}$$

The study conducted by Duong Hung Anh Le et al. provides the following Equation (5) for calculating thermal resistance [34]:

$$R = \frac{L}{k} \tag{5}$$

In accordance with the previously cited studies, Q represents the heat transfer expressed in watts (W), L the thickness of the material in meters (m), A indicates the cross-sectional area expressed in square meters (m^2) and ΔT represents the temperature difference expressed in degrees Celsius (°C) across the sampled material [15,34].

2.4. Statistical Analysis Methodology

The results reported in this study and the related statistical analyses were obtained using R software in the RStudio V.2026.06.0-242 environment. The script is included in the Supplementary Materials (Script S1). This analysis examined the characteristics of the raw materials used for prototyping. For each raw material, the means and standard deviations of the replicates relating to humidity (%), volume (L), and bulk density (kg m^{-3}) were analyzed. The pressure actually exerted on the sample was calculated from the digital

pressure gauge reading. The recorded value was multiplied by the ratio of the hydraulic piston area to the cylinder cap area in contact with the material. Following a similar process, the uncertainty associated with the pressure applied to the sample was calculated by propagating the digital pressure gauge's reading uncertainty. This result, being independent of the type of press used but linked exclusively to the characteristics of the mold, appears to be more representative of the sample.

A similar analysis was performed for the second experiment, but uses the analytically obtained volume, given that the mold size did not vary during the experiment. A variability analysis of the data obtained was then conducted, including the mean, standard deviation, standard error, and 95% confidence interval.

The thermal performance of the bio-based packaging prototypes was analyzed using thresholds to classify and interpret the samples' thermal conductivity, drawing on previous studies. Following the ranges reported for natural bio-based insulation materials, we identified two threshold levels: samples with thermal conductivity values lower than 0.05 W m^{-1} K^{-1} were considered consistent with the good performance range of insulation materials, while values lower than 0.10 W m^{-1} K^{-1} were considered comparable to those reported for natural fiber-based insulation materials and less performing alternative materials [35,36]. Based on these threshold values, the deviation between them and the thermal conductivity recorded for the samples was calculated.

Subsequently, a Spearman correlation matrix was calculated to analyze the monotonic relationships between thermal resistance, thermal conductivity, microwave exposure time, specimen density, applied pressure and biofiber content. Linear regression models were subsequently developed to evaluate the relationships between biofiber content and thermal properties, and between sample density and thermal properties. For each model, regression coefficients, adjusted coefficient of determination (adjusted R^2), root mean square error (RMSE) and mean absolute error (MAE) were calculated.

To study the conductivity and thermal resistance of the samples, an analysis of covariance (ANCOVA) was developed. For this analysis, the biofiber content, the type of material and their interaction were used as predictors, while the duration of exposure to microwaves at T3 was kept fixed. A comparison was also made between whole and broken grape stems to compare the performance of the two grape-stalk forms. Finally, the effect of microwave exposure time on the two distinct waste fiber varieties (C2 and C3) was studied using linear regression. To test non-linear responses, models including quadratic terms were fitted.

3. Results

3.1. Characterization of Raw Materials

For the expanded biopolymer, grape stalks, and spruce bark, the bulk density of the compressed material and the moisture content were measured. The original raw materials measurements are reported in Table S1. The results showed that the biopolymer had a lower bulk density than both stalk types and the bark. In this study, three distinct terms were used to describe the pressure applied to the material. "WIKA pressure" refers to the hydraulic oil pressure of the vertical press, recorded using a WIKA digital pressure gauge. "Cylinder pressure" refers to the pressure directly exerted by the mold plunger on the raw material sample compressed within the cylindrical mold. This mold is used to measure the bulk density of the raw materials. "Parallelepiped pressure" refers to the pressure directly exerted by the mold plunger on the biopackaging sample compressed inside the parallelepiped mold used to produce the samples. The biopolymer achieved a bulk density of 42.36 $\pm$ 0.75 kg m^{-3} at a WIKA pressure of 450 $\pm$ 10 kPa and an estimated cylinder pressure of 44.6 $\pm$ 1 kPa. Due to their lower elasticity and greater tendency to

create macrocavities, the stalks and bark were subjected to a pressure of 760 ± 10 kPa and an estimated cylinder pressure of 75.3 ± 1 kPa. This method yields a bulk density of 399.95 ± 5.45 kg m^{-3} for the bark, 333.57 ± 6.15 kg m^{-3} for the broken stalks, and 333.82 ± 1.91 kg m^{-3} for the whole stalks. The measured volumes were stable across the four tests and are similar to the volumes of the tests carried out with the wooden mold, which equals 0.698 L. Finally, the moisture content (Humidity (%)) of the 4 tests was measured (Table 3).

Table 3. Identification of materials with relative codes, water content (%), weigSht of the sample with the error of the balance (g), pressure registered by WIKA digital pressure gauge and error of measurement (KPa), estimated pressure for the cylindrical mold cap (KPA), volume (L) and bulk density (kg m^{-3}). Moisture content was determined using a gravimetric method; bulk density was determined using a method similar to that described in the study by Chevanan et al. [24].

Material	Humidity (%) μ ± σ	Weight (g)	Pressure WIKA (KPa)	Cylinder Pressure (KPa)	Volume (L) μ ± σ	Bulk Density (kg m^{-3}) μ ± σ
E-PLA (B)	0.90 ± 0.22	30.00 ± 0.01	450 ± 10	44.6 ± 1	0.708 ± 0.013	42.36 ± 0.75
Spruce (C1)	11.85 ± 0.15	279.00 ± 0.01	760 ± 10	75.3 ± 1	0.698 ± 0.010	399.95 ± 5.45
Broken stalks (C2)	11.26 ± 0.16	233.00 ± 0.01	760 ± 10	75.3 ± 1	0.699 ± 0.013	333.57 ± 6.15
Grape stalks (C3)	11.42 ± 0.21	233.00 ± 0.01	760 ± 10	75.3 ± 1	0.698 ± 0.004	333.82 ± 1.91

3.2. Effect of Biomass Type and Content on Specimen Formation

The bark shows excellent performance up to L4, with specimens compact and free of macroscopic fractures. However, beyond this threshold, adhesion between components decreases due to the accumulation of localized bark particles, thereby increasing the tendency to break.

To evaluate the cohesion of the pure bark, a specimen composed entirely of bark was also prepared; despite its compact appearance, it proved extremely fragile, easily disintegrating under minimal stress due to poor adhesion between the particles.

Grape stalks exhibited greater apparent cohesion than bark, yielding compact, solid specimens even at high concentrations, up to L10. However, even in this case, mixing with the biopolymer was difficult: the expanded biopolymer particles tend to infiltrate between the branches and accumulate at the bottom of the sample, leading to an uneven distribution. To address this problem, a test piece was made using C2 to reduce branching and improve mixture homogeneity. However, the modification did not lead to a significant improvement in material distribution.

3.3. Thermal Characterization by Treatment Duration

To test the response of the C3 samples to two biofiber levels, four exposure times (T3, T5, T7, and T9) were evaluated at two biofiber concentrations (L4 and L7). The raw specimen measurements are reported in Table S2. When the two datasets were analyzed separately by biofiber concentration, L4 samples showed lower thermal conductivity than L7 samples. Thermal conductivity of L4 ranged from a minimum of 0.0499 ± 0.0022 W m^{-1} K^{-1} at T3 to a maximum of 0.0528 ± 0.0033 W m^{-1} K^{-1} at T9. Thermal conductivity of L7 ranged from a minimum of 0.0616 ± 0.0022 W m^{-1} K^{-1} at T5 and a maximum of 0.0659 ± 0.0034 W m^{-1} K^{-1} at T3. Thermal resistance of L4, it ranged from a maximum of 1.1231 ± 0.0754 m^2 K W^{-1} at T3 and a minimum of 1.0605 ± 0.0890 m^2 K W^{-1} at T9. The thermal resistance of L7, however, ranged from a maximum of 0.9190 ± 0.0255 m^2 K W^{-1} at T5 and a minimum of 0.8509 ± 0.0467 m^2 K W^{-1} at T3 (Table 4).

Table 4. Thermal conductivity (W m^{-1} K^{-1}), resistance (m^2 K W^{-1}) and density (kg m^{-3}) values of the tests, which were subjected to different thermal treatment times, were as follows: 6 min (T3), 8 min (T5), 10 min (T7), and 12 min (T9). Grape stalks (C3) of 40% and 70% were included in the examined samples. The thermal value of the specimen composed entirely of expanded biopolymer (T3_B_L0) was reported for comparison.

Specimens	Thermal Conductivity (W m^{-1} K^{-1}) $\mu \pm \sigma$	Thermal Resistance (m^2 K W^{-1}) $\mu \pm \sigma$	Bulk Density (kg m^{-3}) $\mu \pm \sigma$	Parallelepiped Pressure (kPa) $\mu \pm \sigma$
T3_B_L0	0.0350 ± 0.0008	1.5047 ± 0.0343	42.24 ± 0.09	45.83 ± 0.57
T3_C3_L4	0.0499 ± 0.0022	1.1231 ± 0.0754	158.45 ± 0.51	51.43 ± 3.57
T5_C3_L4	0.0513 ± 0.0031	1.0922 ± 0.0869	157.82 ± 0.16	47.81 ± 3.18
T7_C3_L4	0.0522 ± 0.0034	1.0742 ± 0.0905	157.70 ± 0.22	48.14 ± 2.06
T9_C3_L4	0.0528 ± 0.0033	1.0605 ± 0.0890	157.59 ± 0.19	48.47 ± 2.62
T3_C3_L7	0.0659 ± 0.0034	0.8509 ± 0.0467	244.99 ± 0.50	60.99 ± 0.57
T5_C3_L7	0.0616 ± 0.0022	0.9190 ± 0.0255	244.21 ± 0.46	58.69 ± 4.46
T7_C3_L7	0.0635 ± 0.0021	0.8783 ± 0.0458	243.37 ± 0.60	63.30 ± 3.43
T9_C3_L7	0.0647 ± 0.0017	0.8680 ± 0.0230	241.95 ± 0.25	61.65 ± 1.51

The same distinction between L4 and L7 was also applied to the bulk density and the pressure exerted by the mold cap on the sample. These values were then transformed to obtain the pressure exerted by the mold plug directly on the sample by multiplying the pressure recorded by the WIKA pressure gauge by the ratio of the area of the press piston to that of the mold plug. For L4, parallelepiped pressure ranged from a minimum of 47.81 ± 3.18 KPa at T5 to a maximum of 51.43 ± 3.57 kPa at T3. For the group of measurements with biofiber content equal to L7, we observe that it ranges from a minimum of 58.69 ± 4.46 kPa for T5 to a maximum of 63.30 ± 3.43 kPa for T7 (Table 4).

3.4. Thermal Performance of Bark and Grape-Stalk-Based Specimens

3.4.1. Thermal Performance: Bark

From heat flow meter tests conducted on specimens L2, L3, L4, and L6 spruce bark (Figure 5), it emerged that as the bark content increases, the thermal conductivity goes from a minimum of 0.0435 ± 0.0006 (L2) to a maximum of 0.0594 ± 0.0036 W m^{-1} K^{-1} (L6). By way of comparison, the thermal conductivity of the test piece made entirely of expanded biopolymer (B) was evaluated and found to be 0.0350 ± 0.0008 W m^{-1} K^{-1} (Table 4).

Figure 5. Image of the sample made from 40% spruce bark (T3_C1_L4). Its production was carried out using a WIKA pressure gauge reading of 760 ± 10 kPa and a 6 min microwave heat treatment (T3).

For completeness, the thermal resistance values measured during the tests with the heat flow meter are reported. Specifically, for L2 to L6, the thermal resistance de-

creases from 1.2971 ± 0.0170 m^2 K W^{-1} to 0.9370 ± 0.0430 m^2 K W^{-1}. For comparison, the thermal resistance of the test piece made of expanded biopolymer was equal to 1.5047 ± 0.0343 m^2 K W^{-1} (Table 5). Bulk density, calculated from the internal volume of the mold and the weight of the specimen, was also reported in the table cited above. The results showed how the bulk density varied from a minimum of 113.59 ± 0.29 kg m^{-3} for L2 to a maximum of 255.37 ± 0.49 kg m^{-3} for sample L6. The value for the pure sample, equal to 42.24 ± 0.09 kg m^{-3}, was used as a reference. Finally, the pressure recorded by the press during sample production was analyzed. The parallelepiped pressure ranged from a minimum of 44.51 ± 1.71 kPa (L2) up to a maximum of 57.04 ± 3.74 kPa (L6). The pressure value of the pure sample, equal to 45.83 ± 0.57 kPa, was reported as a reference (Table 5).

Table 5. Thermal conductivity (W m^{-1} K^{-1}), resistance (m^2 K W^{-1}) and density (kg m^{-3}) values result from thermal tests conducted on specimens containing spruce bark (C1) in different volumetric percentages (L2, L3, L4, L6). For comparison, the thermal value of the specimen composed entirely of expanded biopolymer (T3_B_L0) was also reported.

Specimens	Thermal Conductivity (W m^{-1} K^{-1}) μ ± σ	Thermal Resistance (m^2 K W^{-1}) μ ± σ	Bulk Density (kg m^{-3}) μ ± σ	Parallelepiped Pressure (kPa) μ ± σ
T3_B_L0	0.0350 ± 0.0008	1.5047 ± 0.0343	42.24 ± 0.09	45.83 ± 0.57
T3_C1_L2	0.0435 ± 0.0006	1.2971 ± 0.0170	113.59 ± 0.29	44.51 ± 1.71
T3_C1_L3	0.0464 ± 0.0017	1.2363 ± 0.0572	148.78 ± 0.19	49.78 ± 3.74
T3_C1_L4	0.0547 ± 0.0016	1.0417 ± 0.0325	184.49 ± 0.35	53.74 ± 2.06
T3_C1_L6	0.0594 ± 0.0036	0.9370 ± 0.0430	255.37 ± 0.49	57.04 ± 3.74

3.4.2. Thermal Performance: Grape Stalks

Thermal tests were conducted using a heat flow meter on samples L2, L3, L4, L6, L7, and L10 of the C3 series (Figure 6). The analysis revealed that, as the bio-fiber content increases, thermal conductivity rises from a minimum of 0.0441 ± 0.0029 (L2) to a maximum of 0.0776 ± 0.0030 W m^{-1} K^{-1} (L10). The thermal conductivity of the test piece made with C2 with a concentration of L7 was also reported and it was equal to 0.0629 ± 0.0019 W m^{-1} K^{-1}. This value differs by 4.71% from the value obtained for the C3_L7 samples. For comparison, the thermal conductivity of the test piece made entirely of expanded biopolymer (B) was reported as 0.0350 ± 0.0008 W m^{-1} K^{-1} (Table 6).

Figure 6. Image of the sample made entirely of grape stalks (T3_C3_L10). Its production was carried out using a WIKA pressure gauge reading of 760 ± 10 kPa and a 6 min microwave heat treatment (T3).

Table 6. Thermal conductivity (W m^{-1} K^{-1}), resistance (m^2 K W^{-1}) and density (kg m^{-3}) values from thermal tests conducted on specimens containing grape stalks (C3) in different volumetric percentages (L2, L3, L4, L6, L7 and L10). For comparison, the thermal value of the test piece made with broken grape stalks (C2) and of the test piece composed entirely of expanded biopolymer (T3_B_L0) was also reported.

Specimens	Thermal Conductivity (W m^{-1} K^{-1}) $\mu \pm \sigma$	Thermal Resistance (m^2 K W^{-1}) $\mu \pm \sigma$	Bulk Density (kg m^{-3}) $\mu \pm \sigma$	Parallelepiped Pressure (kPa) $\mu \pm \sigma$
T3_B_L0	0.0350 ± 0.0008	1.5047 ± 0.0343	42.24 ± 0.09	45.83 ± 0.57
T3_C2_L7	0.0629 ± 0.0019	0.8964 ± 0.0348	245.97 ± 0.37	62.31 ± 4.53
T3_C3_L2	0.0441 ± 0.0029	1.2800 ± 0.0897	100.55 ± 0.13	46.82 ± 1.51
T3_C3_L3	0.0454 ± 0.0012	1.2429 ± 0.0523	129.30 ± 0.34	58.03 ± 3.02
T3_C3_L4	0.0499 ± 0.0022	1.1231 ± 0.0754	158.45 ± 0.51	51.43 ± 3.57
T3_C3_L6	0.0586 ± 0.0054	0.9667 ± 0.0992	216.68 ± 0.50	63.30 ± 3.43
T3_C3_L7	0.0659 ± 0.0034	0.8509 ± 0.0467	244.99 ± 0.50	60.99 ± 0.57
T3_C3_L10	0.0776 ± 0.0030	0.7083 ± 0.0195	331.39 ± 1.05	79.13 ± 5.14

For completeness, the thermal resistance values measured during the tests with the heat flow meter are also reported from L2 biomass waste content to L10 for C3. The thermal resistance decreases from 1.2800 ± 0.0897 m^2 K W^{-1} to 0.7083 ± 0.0195 m^2 K W^{-1}. The thermal resistance of the test piece, consisting of L7 with C2 fiber type, was also reported as 0.8964 ± 0.0348 m^2 K W^{-1}. For comparison, the thermal resistance of the test piece made of expanded biopolymer was 1.5047 ± 0.0343 m^2 K W^{-1} (Table 6). The table also shows the bulk density, calculated from the internal volume of the mold and the sample weight. It can be seen that it varies across the samples considered, with values ranging from a minimum of 100.55 ± 0.13 kg m^{-3} for L2 to a maximum of 331.39 ± 1.05 kg m^{-3} for L10. The value of the pure sample, equal to 42.24 ± 0.09 kg m^{-3}, was used as a reference. The sample made with biofiber C2 at a concentration of L7 has a value of 245.97 ± 0.37 kg m^{-3}. This value differs by 0.40% from C3, L7 having a value of 244.99 ± 0.50 kg m^{-3}. Finally, the pressure recorded by the press during sample production was analyzed. Parallelepiped pressure ranged from a minimum of 46.82 ± 1.51 kPa (L2) to a maximum of 79.13 ± 5.14 kPa (L10). The pressure value of the pure sample, equal to 45.83 ± 0.57 kPa, was reported as a reference (Table 6).

4. Discussion

E-PLA, due to its manufacturing process, is highly porous. According to the study conducted by Kasperski et al., air-filled structures in packaging materials can improve thermal insulation because air limits heat transfer [37]. In the present study, this characteristic contributed to reducing heat transfer within the E-PLA structure. This interpretation was consistent with studies on PLA-based biofoams, which have shown that morphology and filler content influence both thermal conductivity and material density [38]. The fully expanded biopolymer specimen (T3_B_L0), used as the common zero-biofiber reference for each type of biofiber, exhibited a lower thermal conductivity (0.0350 ± 0.0008 W m^{-1} K^{-1}); the absence of foreign solid materials prevents thermal bridges, thereby ensuring optimal thermal resistance (1.5047 ± 0.0343 m^2 K W^{-1}).

The thermal performance of the bio-based packaging prototypes was analyzed using thresholds to classify and interpret the samples' thermal conductivity, drawing on previous studies. Following the ranges reported for natural bio-based insulation materials, two interpretative reference levels were adopted: samples with thermal conductivity below 0.05 W m^{-1} K^{-1} were considered to have good insulating performance, whilst those below

0.10 W m^{-1} K^{-1} were considered comparable to those reported for natural fiber-based insulation materials and less performing alternative materials [35,36].

To contextualize the thermal performance of the prototypes analyzed in this study, the measured values were compared with data from the literature regarding commercial polymer foams commonly used as insulation materials. For extruded polystyrene, the thermal conductivity values range from 0.030 to 0.040 W m^{-1} K^{-1}. Expanded polystyrene range from 0.029 and 0.041 W m^{-1} K^{-1}. Polyurethane-based foams range from 0.025 to 0.046 W m^{-1} K^{-1}, depending on factors such as temperature, density, cellular structure and moisture content [39]. In this context, the pure E-PLA sample analyzed in this study proved thermally comparable to conventional foams. The incorporation of spruce bark and grape stalks resulted in an increase in thermal conductivity compared to pure E-PLA; however, the composite samples exhibited values ranging from 0.0435 to 0.0776 W m^{-1} K^{-1}.

The results for bark-containing samples from L2 to L6 highlighted a positive linear increase in thermal conductivity with the volumetric concentration of bark, suggesting that increasing bark incorporation may reduce the insulating performance of the material (Figure 7).

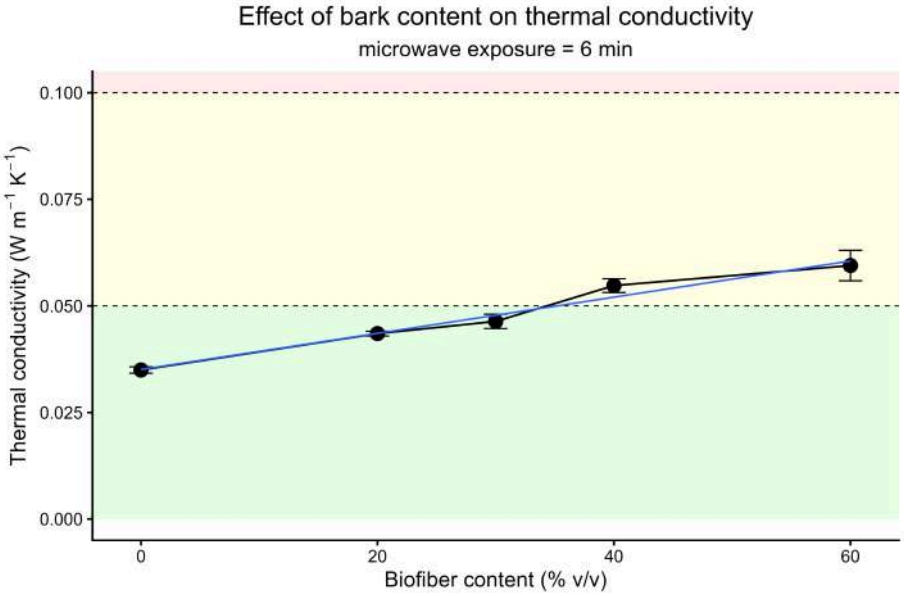

Figure 7. Graphical point representation of the thermal conductivity of samples containing spruce bark as a function of volumetric content, with regression line. This graph analyses samples with a biofiber content ranging from 0% (L0) to 60% (L6). The graph also shows three different bands, green ($k \leq 0.05$ W m^{-1} K^{-1}), yellow ($0.05 < k \leq 0.10$ W m^{-1} K^{-1}), and red ($k > 0.10$ W m^{-1} K^{-1}), which visually classify the insulating quality.

This trend may be related to the higher solid fraction and lower density of E-PLA compared to the waste biofibers considered. This interpretation is consistent with the study by Gößwald et al., which found that spruce bark panels were significantly correlated with density. Thermal conductivity increased from 0.044 W m^{-1} K^{-1} to 0.063 W m^{-1} K^{-1} when going from a density of 164 kg m^{-3} to 276 kg m^{-3} [22]. Despite this significant decrease in performance, samples with varying bark volumes maintained acceptable insulating performance. Upon examining specimen cohesion, it was observed that the sample exhibited sufficient cohesion up to L6. A higher biofiber content led to a progressive decrease in adhesion and facilitated disintegration during handling. During processing using Rstudio statistical software, the following linear model was created (6):

$$k = \beta 1\, Lx + \beta 0 \quad (6)$$

where k represents the thermal conductivity and Lx the volumetric content of the biofiber. In addition to these two variables, the following two coefficients are present: β1 equal to 0.000423 and β0 equal to 0.0351. The regression just described fits the data very well, with an adjusted R^2 of 0.934. Based on this regression, we can state that for every percentage point increase in volumetric bark concentration, the thermal conductivity increases by 0.000423 W m^{-1} K^{-1}.

Analysis of samples containing grape stalks with a volumetric content of up to L10 shows good insulating properties even at high concentrations (Figure 8). These results were consistent with previous research showing that this type of residue can be incorporated as bio-based aggregates. However, the binding mechanism and processing route differ from those used in the present study [20]. The current study indicates that grape stalks maintain relatively good thermal properties and apparent cohesion, likely attributable to their fibrous and compact structure, which can retain air within a dense particle network, although efficacy tends to decline slightly at high concentrations. Compared with the bark, the stalk provided similar stability, albeit with slightly higher insulating performance. Consequently, they are designed as a solution that combines a high material seal with a slight loss of insulating power, even at high biofiber concentrations. During processing using RStudio statistical software, the following linear model was created (7):

$$k = \beta 1\ Lx + \beta 0 \quad (7)$$

where k represents the thermal conductivity and Lx the volumetric content of the biofiber. In addition to these two variables, the following two coefficients are present: β1 equals 0.000431 and β0 equals 0.03408. The regression just described fits the data very well, with an adjusted R^2 of 0.955. Based on this regression, we can state that for every 1 percentage point increase in the volumetric grape stalks concentration, the thermal conductivity increases by 0.000431 W m^{-1} K^{-1}.

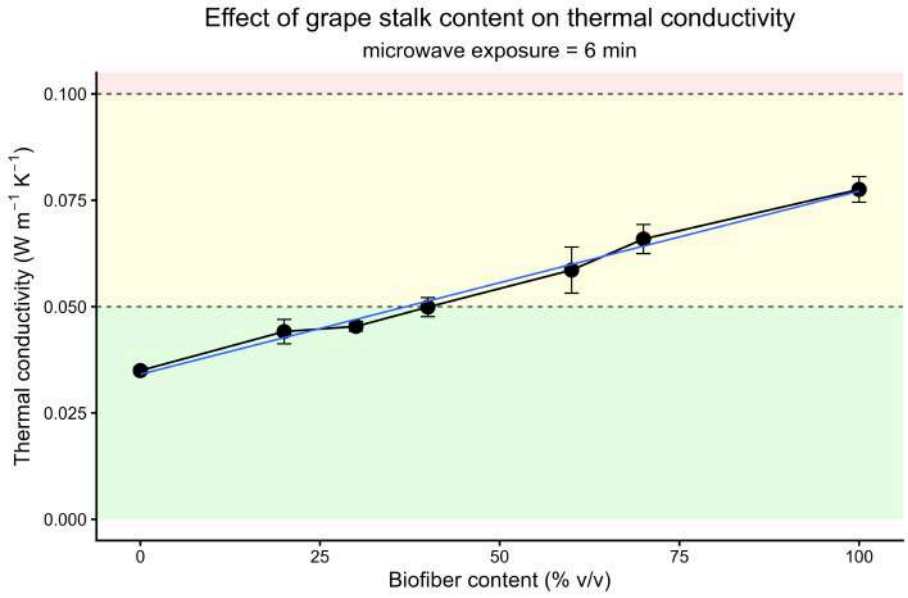

Figure 8. Graphical point representation of the thermal conductivity of samples containing grape stalks as a function of their volumetric content, with regression line. This graph analyses samples with biofiber content ranging from 0% (L0) to 100% (L10). The graph also shows three different bands, green ($k \leq 0.05$ W m^{-1} K^{-1}), yellow ($0.05 < k \leq 0.10$ W m^{-1} K^{-1}), and red ($k > 0.10$ W m^{-1} K^{-1}), which visually classify the insulating quality.

A comparative investigation of the two lignocellulosic biomaterials revealed that grape stalk-based composites showed similar thermal conductivity to bark-based composites (Figure S1). The bark samples exhibited an increase in thermal conductivity from roughly 0.0350 ± 0.0008 (B) to 0.0594 ± 0.0036 W m^{-1} K^{-1} as the bark content rose to 60% (v/v), reflecting an increase of 69.97%. Conversely, grape stalk composites rose from around 0.0350 ± 0.0008 (B) to 0.0776 ± 0.0030 W m^{-1} K^{-1} at 100% (v/v), indicating an increase of 121.83%. Furthermore, at similar intermediate incorporation levels, grape stalk composites exhibited thermal conductivity values 8.83% lower than those of bark-based materials at 40% v/v.

Using the ANCOVA model, we can confirm that biofiber content (Lx) is the dominant factor controlling thermal conductivity (k), producing a highly significant effect ($p < 2 \times 10^{-16}$). Conversely, material type (Cx) is not significant ($p = 0.4295$), nor is the interaction between biofiber content and material type ($p = 0.8503$). This result should be interpreted considering that the two residues used in this study were not tested over the same full concentration range. This is because spruce-bark specimens showed reduced handling integrity at higher biofiber contents. The following equation explain the used model (8):

$$k = \beta 3\, Lx + \beta 2\, Cx + \beta 1\, Lx * Cx + \beta 0 \quad (8)$$

The model demonstrated very high explanatory power, with an adjusted R^2 of 0.952. Supporting this consideration, the predictive error is very low: MAE = 0.00201 W m^{-1} K^{-1} and RMSE = 0.00257 W m^{-1} K^{-1}.

The same predictors were also applied to the ANCOVA model, with thermal resistance as the response variable. As described for thermal conductivity, biofiber content was again highly significant ($p < 2 \times 10^{-16}$). On the other hand, the interaction between material type and biofiber content was only marginal ($p = 0.0635$). The model demonstrates high explanatory power, with an adjusted R^2 of 0.939, an RMSE of 0.0571 m^2 K W^{-1}, and an MAE of 0.0466 m^2 K W^{-1}.

Models based on density (D) and material type (Cx) were also developed. The results obtained are consistent with those previously reported; density is strongly associated with thermal conductivity (k) ($p < 2 \times 10^{-16}$). Material type ($p = 0.0164$) and the interaction between material and density ($p = 0.0172$) were also significant. These results indicate that the reported relationship differs significantly between the two groups of materials. The model showed high explanatory power, with an adjusted R^2 of 0.952 and an RMSE of 0.00256 W m^{-1} K^{-1}. The equation for the model used is as follows (9):

$$k = \beta 3\, D + \beta 2\, Cx + \beta 1\, D * Cx + \beta 0 \quad (9)$$

Using the same predictors, a model with thermal resistance as the response variable was generated. In this case, density also appears to be highly associated ($p < 2 \times 10^{-16}$). On the other hand, material type ($p = 0.103$) and the interaction between material and density ($p = 0.885$) were not significant. The model showed high explanatory power, with an adjusted R^2 of 0.940 and an RMSE of 0.0568 m^2 K W^{-1}.

The comparison between broken and whole grape stalks (Figure 9) revealed that greater fragmentation did not enhance the homogeneity and properties of the matrix. This result suggests that particle morphology and aggregate-matrix distribution are critical factors, particularly as the expanded PLA filters through the biofiber, utilizing the macrocavities present prior to compression [20,38].

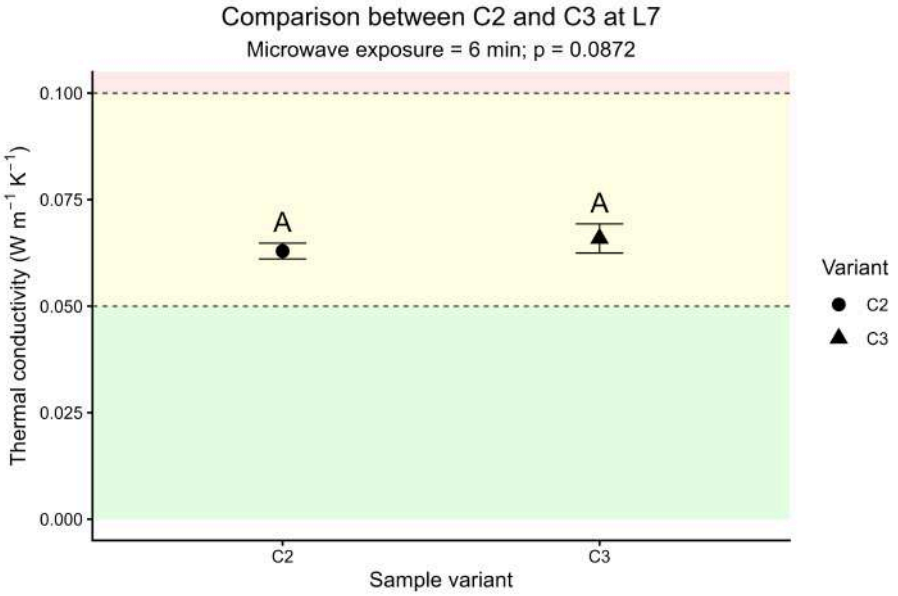

Figure 9. Graphical point representation of the statistical comparison of thermal conductivity for whole stalk (C3) and broken stalk (C2) samples for a volumetric concentration of 70% with respect to the polymer component (L7). The graph also shows three different bands, green ($k \leq 0.05$ W m^{-1} K^{-1}), yellow ($0.05 < k \leq 0.10$ W m^{-1} K^{-1}), and red ($k > 0.10$ W m^{-1} K^{-1}), which visually classify the insulating quality. The letters in the graph represent any statistical difference between the two cases. In this graph, since the letters are the same, grape stalk breakage does not have a statistically significant effect.

Statistical comparisons between C3 and C2 confirmed that fiber breakage had a limited effect on thermal response. C3 samples showed an average thermal conductivity of 0.0659 W m^{-1} K^{-1}, slightly higher than that of C2 (0.0629 W m^{-1} K^{-1}). However, these deviations were not significant for the *t*-test analysis ($p = 0.0872$). Consequently, C2 and C3 cannot be clearly distinguished in terms of conductive behavior. These analyses showed that grape stem fragmentation did not produce a significant improvement in thermal conductivity.

By analyzing samples comprising L4 and L7 grape stalks by volume, we observed minor effects of heat treatment time (Figure 10). In detail, by varying the duration of the heat treatment, the insulating performance at L4 was moderately influenced, as demonstrated by a slight increase in thermal conductivity (from 0.0499 ± 0.0022 to 0.0528 ± 0.0033 W m^{-1} K^{-1}) and a reduction in thermal resistance (from 1.1231 ± 0.0754 to 1.0605 ± 0.0890 m^2 K W^{-1}) as the time increases, from T3 to T9 observing a variation in values equal to 5.81–5.57%.

The statistical models used for L4 confirm that we should interpret this trend with caution. The linear model, reported below (10), showed a positive trend ($\beta 1 = 0.000482$), with a non-significant relationship between microwave exposure time (Tx) and thermal conductivity (k) ($p = 0.207$). Due to the low variability of the response variable, the model produced an adjusted R^2 of 0.070 and an RMSE of 0.00252 W m^{-1} K^{-1}.

$$k = \beta 1\, Tx + \beta 0 \quad (10)$$

A quadratic model was also applied, but it did not provide significant results. This model presented a similar RMSE (0.00251 W m^{-1} K^{-1}) but with a negative adjusted R^2. The same behavior was also observed for thermal resistance. The slope of the linear regressor was negative ($\beta 1 = -0.0103$) with low significance (adjusted $R^2 = 0.007$, RMSE = 0.0701 m^2 K W^{-1}), while the quadratic regressor performance was similar.

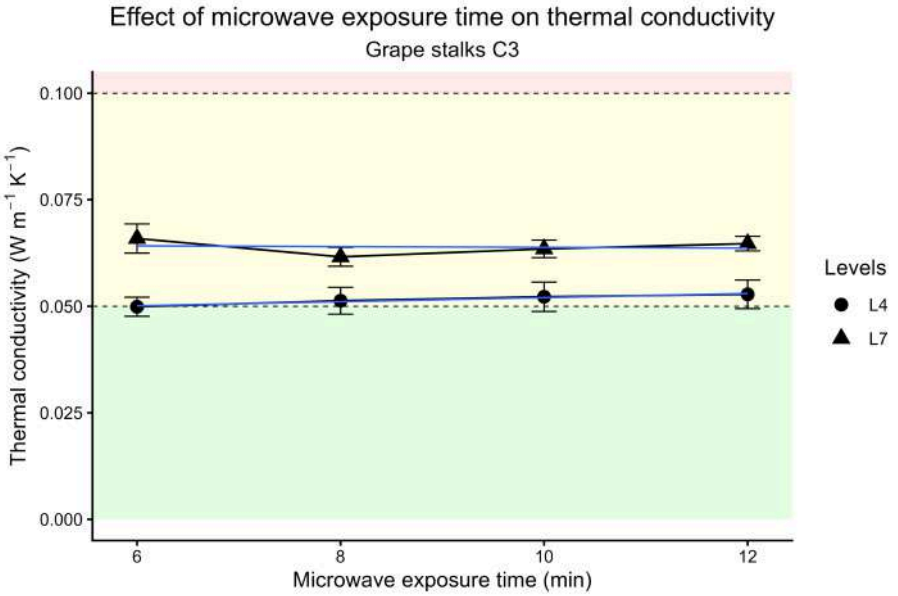

Figure 10. Graphical point representation of the thermal conductivity of samples containing grapevine stems (C3) for heat treatments of 6 (T3), 8 (T5), 10 (T7), and 12 (T9) minutes, with regression lines. These heat treatments were performed using microwaves. This analysis was applied to two levels of biofiber volumetric concentration: 40% (L4) and 70% (L7). The graph also shows three different bands, green ($k \leq 0.05$ W m^{-1} K^{-1}), yellow ($0.05 < k \leq 0.10$ W m^{-1} K^{-1}), and red ($k > 0.10$ W m^{-1} K^{-1}), which visually classify the insulating quality.

Increasing the concentration of biofiber at L7 does not yield further marked variations. A slight variation in thermal conductivity can be observed between T3 to T5: thermal conductivity decreases of 6.53% (from 0.0659 ± 0.0034 to 0.0616 ± 0.0022 W m^{-1} K^{-1}) and thermal resistance increases of 8.01% (from 0.8509 ± 0.0467 to 0.9190 ± 0.0255 m^2 K W^{-1}). This suggest a possible improved cohesion between the expanded biopolymer and the lignocellulosic fraction at the expense of higher energy consumption due to the longer treatment with microwaves, equal to 33.33%. A slight dwindling in performance was observed for heat treatments lasting T7 and T9: thermal conductivity increased (from 0.0635 ± 0.0021 to 0.0647 ± 0.0017 W m^{-1} K^{-1}), and thermal resistance decreased (from 0.8783 ± 0.0458 to 0.8680 ± 0.0230 m^2 K W^{-1}). This specific case suggests a possible pattern correlating varying microwave exposure times with changes in thermal insulation. Under the conditions tested, heat treatment up to T5 provides slight benefits at the expense of increased energy consumption.

Applying the linear model shown below (11) to the L7 samples, we found no significant linear effect of microwave exposure time (Tx). The model showed a non-significant relationship between the dependent and independent variables ($p = 0.814$) and a very low slope ($\beta 1 = -0.0000867$). Furthermore, the curve had an adjusted R^2 of -0.094 and an RMSE of 0.00254 W m^{-1} K^{-1}.

$$k = \beta 1\, Tx + \beta 0 \quad (11)$$

The quadratic model had a slightly better but not significant fit, as the adjusted R^2 increased from -0.094 to 0.146 and the RMSE decreased from 0.00254 to 0.00213 W m^{-1} K^{-1}. The same behavior was also observed for thermal resistance. The slope of the linear regressor was slightly positive ($\beta 1 = 0.000535$) but remained low in significance (adjusted $R^2 = -0.099$, RMSE = 0.0392 m^2 K W^{-1}), while the quadratic regressor performed slightly better but not significantly.

A Spearman correlation was applied to this study (Figure 11). This correlation confirmed the importance of biofiber content in determining the thermal behavior of the

samples. This parameter showed a strong positive correlation with thermal conductivity ($\rho = 0.95$) and a strong negative correlation with thermal resistance ($\rho = -0.95$). Sample density followed the same trend, showing a positive correlation with thermal conductivity ($\rho = 0.90$) and a negative correlation with thermal resistance ($\rho = -0.90$). Conversely, microwave exposure time showed a correlation with the same sign but a weaker correlation with thermal conductivity ($\rho = 0.26$) and thermal resistance ($\rho = -0.26$).

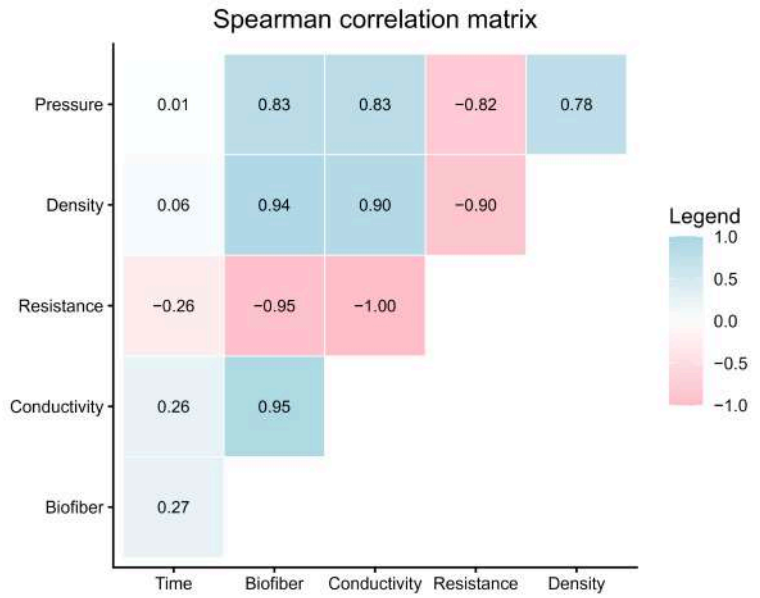

Figure 11. Graphical representation of the Spearman correlation matrix. The matrix shows the strength of the correlation between two variables and whether it is direct (blue box) or inverse (red box).

5. Conclusions

This study evaluated the thermal properties of new bio-based packaging prototypes based on expanded PLA and agroforestry residues used in a raw or minimally processed form. Specifically, vine stalks and spruce bark were used as waste woody biofibers.

The pure E-PLA sample demonstrated the best insulation performance. The incorporation of waste biofibers resulted in a statistically supported increase in thermal conductivity and a decrease in thermal resistance. These performance losses were limited, allowing the samples derived from the various blends to maintain thermal conductivity values of practical interest for preliminary thermal-insulation functions in bio-based packaging [35,36]. This trend was little affected by the type of plant fiber used, but was more strongly influenced by the increase in the waste fraction relative to E-PLA and by the associated increase in specimen density.

The main difference found between the two biofibers examined was related to specimen formation and qualitative handling behavior. The bark samples maintained good properties up to intermediate biofiber concentrations. In this study, increasing spruce bark content reduced the specimens' qualitative handling integrity. This phenomenon was not observed in the samples made from grape stalks. Samples made from this type of biofiber exhibited good structure, without macroscopic fractures, even in pure samples.

In this study, a comparison was conducted between whole stalks and fragmented stalks, but no significant differences were found. The study also varied the microwave exposure times and the method used to bond the particles and fibers in the sample. Varying the heat treatment times did not result in appreciable changes in thermal conductivity or thermal resistance.

Overall, the results from this study suggest the possibility of producing packaging prototypes containing blends of biofibers and E-PLA, thereby valorizing agroforestry residues within bio-based packaging applications. However, the present study does not provide a comprehensive assessment of packaging performance and should be interpreted as preliminary thermal characterization. Future studies should include microstructural characterization, moisture resistance and dimensional stability assessments, mechanical testing, cost analysis and life-cycle assessment before the industrial applicability of these prototypes can be fully evaluated. Future studies should also evaluate the thermal response over a wider range of operating temperatures in real-world environments, including scenarios involving frozen products, the cold chain, and hot filling but also mold-filling uniformity, process reproducibility under industrially relevant manufacturing conditions, specimen size and edge effects.

Supplementary Materials: The following supporting information can be downloaded at: https://www.mdpi.com/article/10.3390/recycling11070123/s1, Figure S1: Global graph showing the thermal conductivity of two biofibers of different nature, vine stalk and spruce bark, as their volumetric concentration within the samples varies; Table S1: Table showing the data of the raw materials used in the statistical analysis; Table S2: Table showing the raw data of the biopackaging samples made in this study; Script S1: Script relating to the statistical analysis conducted to obtain the outputs of this study.

Author Contributions: Conceptualization, N.R., D.S., F.R. and G.R.; methodology, N.R., F.R., D.S., G.R. and G.B.; software, N.R.; validation, N.R., J.S., D.S. and L.C.; formal analysis, N.R. and C.P.; investigation, N.R., C.P., J.S. and D.S.; resources, N.R., D.S., G.R. and L.C.; data curation, N.R., D.S. and G.R.; writing—original draft preparation, N.R., C.P., D.S. and A.P.; writing—review and editing, N.R., C.P., D.S., A.P., G.R. and L.C.; visualization, N.R.; supervision, D.S., G.R., L.C. and G.B.; project administration, G.R.; funding acquisition, G.R., F.R. and D.S. All authors have read and agreed to the published version of the manuscript.

Funding: This study was carried out within the Agritech National Research Center and funded by the European Union Next-Generation EU Piano Nazionale di Ripresa e Resilienza (PNRR)—Missione 4 Componente 2, Investimento 1.4, grant number D.D. 1032 17/06/2022, CN00000022 and the Erasmus+ Programme of the European Union under the VTSkills project grant number 101139985.

Data Availability Statement: The original contributions presented in this study are included in the article and Supplementary Material. Further inquiries can be directed to the corresponding author.

Conflicts of Interest: Jessica Scriva is an employee of Bluebiloba Startup Innovativa S.r.l. The other authors declare no conflicts of interest. Bluebiloba Startup Innovativa S.r.l. had no role in the design of the study; in the collection, analyses, or interpretation of data; in the writing of the manuscript; or in the decision to publish the results.

Abbreviations

The following abbreviations are used in this manuscript:

A	Cross-sectional area
A1	Hydraulic piston striking area
A2	Cylinder or mold cap area
ANCOVA	Analysis of covariance
ASTM	American Society for Testing and Materials
B	Expanded biopolymer
Cx	Generic biofiber code
C1	Spruce bark
C2	Broken grape stalks

C3	Whole grape stalks
D	Specimen density
E-PLA	Expanded polylactic acid
EU	European Union
HFM	Heat flow meter
ISO	International Organization for Standardization
k	Thermal conductivity
L	Specimen thickness
Lx	Volumetric ratio level code
MAE	Mean absolute error
MC	Moisture content
PBAT	Polybutylene adipate terephthalate
PEG	Polyethylene glycol
PHA	Polyhydroxyalkanoates
PLA	Polylactic acid
P	Applied pressure
PNRR	Piano Nazionale di Ripresa e Resilienza
P1	Pressure recorded by the digital pressure gauge
P2	Estimated pressure exerted on the material
Q	Heat transfer
R	Thermal resistance
RMSE	Root mean square error
Tx	Thermal treatment time code
UTM	Universal Testing Machine
ΔT	Temperature difference
μ	Mean
σ	Standard deviation
ρ	Spearman correlation coefficient

References

1. Geissdoerfer, M.; Savaget, P.; Bocken, N.M.P.; Hultink, E.J. The circular economy—A new sustainability paradigm? *J. Clean. Prod.* **2017**, *143*, 757–768. [CrossRef]
2. Lebreton, L.; Andrady, A. Future scenarios of global plastic waste generation and disposal. *Palgrave Commun.* **2019**, *5*, 6. [CrossRef]
3. Diggle, A.; Walker, T.R. Environmental and economic impacts of mismanaged plastics and measures for mitigation. *Environments* **2022**, *9*, 15. [CrossRef]
4. Hurley, R.; Horton, A.; Lusher, A.; Nizzetto, L. Plastic waste in the terrestrial environment. In *Plastic Waste and Recycling*; Elsevier: Amsterdam, The Netherlands, 2020; pp. 163–193. [CrossRef]
5. Zhang, J.; Ren, S.; Xu, W.; Liang, C.; Li, J.; Zhang, H.; Li, Y.; Liu, X.; Jones, D.L.; Chadwick, D.R.; et al. Effects of plastic residues and microplastics on soil ecosystems: A global meta-analysis. *J. Hazard. Mater.* **2022**, *435*, 129065. [CrossRef] [PubMed]
6. Kirchherr, J.; Reike, D.; Hekkert, M. Conceptualizing the circular economy: An analysis of 114 definitions. *Resour. Conserv. Recycl.* **2017**, *127*, 221–232. [CrossRef]
7. Merli, R.; Preziosi, M.; Acampora, A. How do scholars approach the circular economy? A systematic literature review. *J. Clean. Prod.* **2018**, *178*, 703–722. [CrossRef]
8. Morseletto, P. Targets for a circular economy. *Resour. Conserv. Recycl.* **2020**, *153*, 104553. [CrossRef]
9. Geyer, R.; Jambeck, J.R.; Lavender Law, K. Production, use, and fate of all plastics ever made. *Sci. Adv.* **2017**, *3*, e1700782. [CrossRef] [PubMed]
10. Plastics Europe. Plastics—The Fast Facts 2024. Available online: https://plasticseurope.org/knowledge-hub/plastics-the-fast-facts-2024/ (accessed on 3 June 2026).
11. Vert, M.; Doi, Y.; Hellwich, K.-H.; Hess, M.; Hodge, P.; Kubisa, P.; Rinaudo, M.; Schué, F. Terminology for biorelated polymers and applications (IUPAC Recommendations 2012). *Pure Appl. Chem.* **2012**, *84*, 377–410. [CrossRef]
12. Ghasemlou, M.; Barrow, C.J.; Adhikari, B. The future of bioplastics in food packaging: An industrial perspective. *Food Packag. Shelf Life* **2024**, *43*, 101279. [CrossRef]

13. Gururani, P.; Bhatnagar, P.; Dogra, P.; Joshi, H.C.; Chauhan, P.K.; Vlaskin, M.S.; Joshi, N.C.; Kurbatova, A.; Irina, A.; Kumar, V. Bio-based food packaging materials: A sustainable and holistic approach for cleaner environment—A review. *Curr. Res. Green Sustain. Chem.* **2023**, *7*, 100384. [CrossRef]
14. Reichert, C.L.; Bugnicourt, E.; Coltelli, M.-B.; Cinelli, P.; Lazzeri, A.; Canesi, I.; Braca, F.; Monje Martínez, B.; Alonso, R.; Agostinis, L.; et al. Bio-based packaging: Materials, modifications, industrial applications and sustainability. *Polymers* **2020**, *12*, 1558. [CrossRef] [PubMed]
15. Raja, P.; Murugan, V.; Ravichandran, S.; Behera, L.; Mensah, R.A.; Mani, S.; Kasi, A.; Balasubramanian, K.B.N.; Sas, G.; Vahabi, H.; et al. A review of sustainable bio-based insulation materials for energy-efficient buildings. *Macromol. Mater. Eng.* **2023**, *308*, 2300086. [CrossRef]
16. Hong, J.; Lee, J.; Kim, S.K.; Son, D.; Kang, D.; Shim, J.K. Enhancing thermal insulation property and flexibility of starch/poly(butylene adipate terephthalate) (PBAT) blend foam by improving rheological properties. *Polymers* **2025**, *17*, 138. [CrossRef] [PubMed]
17. Baniasadi, H.; Abidnejad, R.; Cruz, C.D.; Fathi, Z.; Tammela, P.; Kontturi, E.; Lizundia, E. Sustainable multifunctional foams for cold-chain packaging: Stabilizing polyethylene glycol with cellulose and pomegranate peel for antibacterial protection and temperature control. *Sustain. Mater. Technol.* **2025**, *43*, e01312. [CrossRef]
18. Xie, A.; Du, H.; Mohapatra, S.; Liu, K.; Yang, J.; Oh, J.-H.; Li, M.; Zhang, Y.; Gao, M.; Gunasekaran, S.; et al. Engineering robust, hierarchical, and biodegradable cellulose foams for smart packaging. *Chem. Eng. J.* **2025**, *523*, 168461. [CrossRef]
19. Kim, J.; Lee, J.; Lee, S.; Kwon, O.; Lee, J.; Kim, J. Enhanced biodegradability and thermal insulation capability of polylactic acid reinforced with calcium-crosslinked orange peel biochar. *Ind. Crops Prod.* **2025**, *226*, 120666. [CrossRef]
20. Blasi, A.; Verardi, A.; Lopresto, C.G.; Siciliano, S.; Sangiorgio, P. Lignocellulosic agricultural waste valorization to obtain valuable products: An overview. *Recycling* **2023**, *8*, 61. [CrossRef]
21. San Martin, D.; Ibarruri, J.; Luengo, N.; Ferrer, J.; García-Rodríguez, A.; Goiri, I.; Atxaerandio, R.; Zufía, J.; Sáez de Cámara, E.; Iñarra, B. Evaluation of valorisation strategies to improve grape stems' nutritional value as an ingredient for ruminants' diets. *Sustainability* **2023**, *15*, 11951. [CrossRef]
22. Badouard, C.; Bogard, F.; Bliard, C.; Lachi, M.; Abbes, B.; Polidori, G. Development and characterization of viticulture by-products for building applications. *Constr. Build. Mater.* **2021**, *302*, 124142. [CrossRef]
23. Feng, S.; Cheng, S.; Yuan, Z.; Leitch, M.; Xu, C.C. Valorization of bark for chemicals and materials: A review. *Renew. Sustain. Energy Rev.* **2013**, *26*, 560–578. [CrossRef]
24. Gößwald, J.; Barbu, M.-C.; Petutschnigg, A.; Tudor, E.M. Binderless thermal insulation panels made of spruce bark fibres. *Polymers* **2021**, *13*, 1799. [CrossRef] [PubMed]
25. Martynenko, A. True, particle, and bulk density of shrinkable biomaterials: Evaluation from drying experiments. *Dry. Technol.* **2014**, *32*, 1319–1325. [CrossRef]
26. Chevanan, N.; Womac, A.R.; Bitra, V.S.P.; Igathinathane, C.; Yang, Y.T.; Miu, P.I.; Sokhansanj, S. Bulk density and compaction behavior of knife mill chopped switchgrass, wheat straw, and corn stover. *Bioresour. Technol.* **2010**, *101*, 207–214. [CrossRef] [PubMed]
27. Swetha, T.A.; Bora, A.; Mohanrasu, K.; Balaji, P.; Raja, R.; Ponnuchamy, K.; Muthusamy, G.; Arun, A. A comprehensive review on polylactic acid (PLA)—Synthesis, processing and application in food packaging. *Int. J. Biol. Macromol.* **2023**, *234*, 123715. [CrossRef] [PubMed]
28. Saccani, A.; Fiorini, M.; Burzotta, G. Sustainable bio-composites obtained from recycling post-industrial PLA and fillers derived from coffee production. *Recycling* **2022**, *7*, 89. [CrossRef]
29. BEWI. BioFoam. Available online: https://bewi.com/wp-content/uploads/2021/01/BioFoam-Flyer-2022.pdf (accessed on 3 June 2026).
30. Ilek, A.; Siegert, C.M.; Wade, A. Hygroscopic contributions to bark water storage and controls exerted by internal bark structure over water vapor absorption. *Trees* **2021**, *35*, 831–843. [CrossRef]
31. Ilic, D.; Williams, K.C.; Ellis, D. Assessment of biomass bulk elastic response to consolidation. *Chem. Eng. Res. Des.* **2018**, *135*, 185–196. [CrossRef]
32. *ASTM C518-21*; Standard Test Method for Steady-State Thermal Transmission Properties by Means of the Heat Flow Meter Apparatus. ASTM International: West Conshohocken, PA, USA, 2021. [CrossRef]
33. *ISO 8301:1991*; Thermal Insulation—Determination of Steady-State Thermal Resistance and Related Properties—Heat Flow Meter Apparatus. International Organization for Standardization: Geneva, Switzerland, 1991.
34. Le, D.H.A.; Pásztory, Z. Experimental study of thermal resistance values of natural fiber insulating materials under different mean temperatures. *South-East Eur. For.* **2023**, *14*, 93–99. [CrossRef]
35. Cosentino, L.; Fernandes, J.; Mateus, R. A review of natural bio-based insulation materials. *Energies* **2023**, *16*, 4676. [CrossRef]
36. Hung Anh, L.D.; Pásztory, Z. An overview of factors influencing thermal conductivity of building insulation materials. *J. Build. Eng.* **2021**, *44*, 102604. [CrossRef]

37. Kasperski, J.; Grabowska, B. Optimizing the thermal effectiveness of an insulation wrap with internal folded polypropylene film for the transportation of frozen food. *Int. J. Refrig.* **2016**, *67*, 42–53. [CrossRef]
38. Oluwabunmi, K.; D'Souza, N.A.; Zhao, W.; Choi, T.-Y.; Theyson, T. Compostable, fully biobased foams using PLA and micro cellulose for zero energy buildings. *Sci. Rep.* **2020**, *10*, 17771. [CrossRef] [PubMed]
39. Ali, A.; Issa, A.; Elshaer, A. A comprehensive review and recent trends in thermal insulation materials for energy conservation in buildings. *Sustainability* **2024**, *16*, 8782. [CrossRef]